Available online at www.sciencedirect.com

ScienceDirect

Current Opinion in
Colloid & Interface Science

Classical atomistic simulations of protein adsorption on carbon nanomaterials

Fabio Ganazzoli and Giuseppina Raffaini

Abstract

Carbon nanomaterials are receiving an increasingly large interest in a variety of fields, including also nanomedicine. In this area, much attention is devoted to investigating and modeling the behavior of these nanomaterials when they interact with biological fluids and with biological macromolecules, in particular proteins and oligopeptides. The interaction with these molecules is in fact crucial to understand and predict the efficacy of nanomaterials as drug carriers or therapeutic agents as well as their potential toxicity when they occupy the active site of a protein or severely affect the secondary and tertiary structure, or even the local dynamics, thus inhibiting their biological function. In this review, therefore, we describe the most recent work carried out in the last few years to model the interaction between carbon nanomaterials, either pristine or functionalized, and proteins or oligopeptides using classical atomistic methods, mainly molecular dynamics simulations. The attention is focused on 0-dimensional fullerenes, mainly C_{60}, on 1-dimensional carbon nanotubes, mostly the single-walled armchair and some chiral ones, and on 2-dimensional graphene and graphyne, the latter containing also *sp* hybridized atoms in addition to the sp^2 ones common to the other carbon nanomaterials.

Addresses

Dipartimento di Chimica, Materiali ed Ingegneria Chimica "G. Natta", Politecnico di Milano, via L. Mancinelli 7, 20131 Milano, Italy

Corresponding author: Ganazzoli, Fabio (fabio.ganazzoli@polimi.it)

Current Opinion in Colloid & Interface Science 2019, **41**:11–26

This review comes from a themed issue on **Theory and Simulation**

Edited by **Nily Dan** and **Zbigniew damczyk**

For a complete overview see the Issue and the Editorial

https://doi.org/10.1016/j.cocis.2018.11.008

Keywords

Molecular dynamics, Atomistic simulations, Carbon nanomaterials, Protein adsorption, Fullerenes, Carbon nanotubes, Graphene, Graphyne.

Introduction

Carbon nanostructured materials have attracted a huge interest in recent years in a variety of fields, for instance in the area of nanomedicine [1]. These applications require the direct interaction of these nanomaterials with biological molecules such as lipids, DNA and in particular proteins (see for instance Ref. [2]). In fact, carbon nanomaterials can strongly interact with proteins, thus affecting their structure, hence their biological activity, either because they may occupy the active sites inhibiting their enzymatic activity, or because they may modify their secondary and/or tertiary structure. In this way, depending on the involved protein they can be very effective therapeutic agents, or else display highly toxic effects. Besides, the carbon nanomaterials are also actively investigated as drug or gene carriers. The detailed experimental study of these interactions is very difficult, and therefore much work is currently being done by atomistic computer simulations. For instance, various review papers recently addressed the simulation tools that were applied to investigate the nanotoxicology of carbon nanomaterials at the molecular level, often together with some experimental data (see for instance Refs. [3,4]), modeling the physical driving forces for the interaction of proteins with carbon nanotubes, eventually responsible for the observed nanotoxicity [5]. Other recent reviews described the non-covalent protein functionalization of carbon nanotubes for optical biosensing and biodelivery applications [6] and relevant computational studies involving classical and quantum methods of individual aminoacids, peptides and proteins on graphitic nanomaterials up to 2014 [7]. Details were given of the physico-chemical modes of adsorption and the driving forces leading to the non-covalent hybrid complexes, but did focus on purely carbon materials, not considering for instance those simulations dealing with the functionalized surfaces currently used in experimental work.

In fact, the carbon nanomaterials are strongly hydrophobic and form insoluble aggregates in water, while suitably derivatized materials can display a large solubility in polar environments such as the physiological fluids, and in particular in water: for instance, OH groups can strongly modify the hydrophobic behavior of the pristine materials enhancing to various degrees their hydrophilicity, depending on the degree of functionalization. As a result, the interaction of these nanoparticles with biological molecules, be they proteins, lipids or DNA, can also be largely affected and controlled.

Figure 1

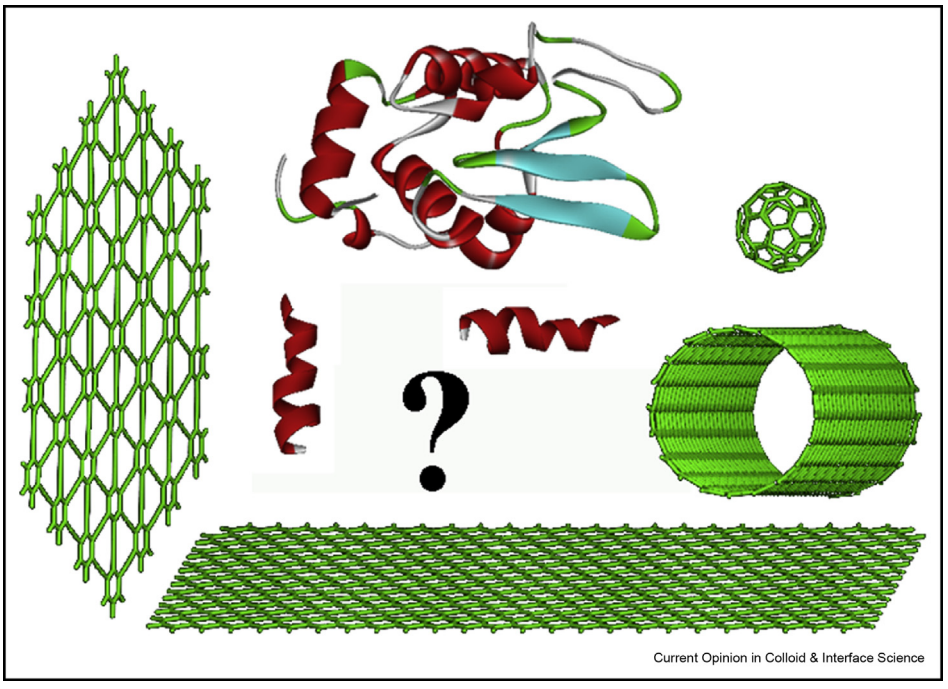

The systems considered in this review comprise proteins or oligopeptides usually structured in α-helices and/or β sheet (above) interacting with carbon nanomaterials such as 2D graphyne or a graphene sheets, 1D carbon nanotubes and 0D fullerenes shown below from left to right.

In the following, we will review further simulation results obtained in the very last few years for oligopeptides or whole proteins, or at least protein subdomains of different structures and biological functions interacting with nanostructured carbon materials, either in their pristine state or functionalized with appropriate moieties. In particular, the carbon nanomaterials currently investigated comprise, in their pristine state *i*) the 0-dimensional fullerene systems, such as the most popular C_{60}, but also the larger-sized C_{70} and even larger fullerenes, having both five- and six-membered rings with sp^2 atoms; *ii*) the 1-dimensional carbon nanotubes (or CNT), formed by six-membered aromatic rings again with sp^2 atoms having largely different diameters, characterized by the chiral vector indices (n, m): most studies considered for simplicity the armchair CNT, where $n = m$, but in one instance chiral nanotubes with $n \neq m$ were also modeled for specific purposes; *iii*) the 2-dimensional nanosheet surfaces, having a single-atom thickness: *a*) in most cases, a graphene plane formed by six-membered aromatic rings (CNT's may thus be viewed as formed by differently rolling up a graphene sheet); *b*) in some instances, a graphyne plane formed by six-membered aromatic rings with sp^2 atoms connected by a single −C≡C- groups with sp atoms (thus forming a 2-D triangular lattice where the vertices are defined by the aromatic rings, and the edges by a single alkyne group). Let us point out that unless otherwise stated the atomistic simulations were carried out by the most popular molecular dynamics (MD) methods in explicit water for tens or for one or two hundreds of nanoseconds, which often leads to a reasonable equilibration (Figure 1).

Pristine carbon nanomaterials with single proteins

Fullerenes

Much work has been carried out in the present decade on the interaction of C_{60} and, to some extent, of C_{70} with proteins. In this context, the screening procedure proposed a few years ago is of great importance because it allows a fast and statistically reliable procedure to find both the preferred fullerenes and the likely interaction sites [8••,9] (see also ref. [7]). In these papers, a systematic computational approach was adopted to study the fullerene−protein interactions using the PDTD, a protein database for drug target identification [10]. The screening [8] was carried out with C_{60} at first using a two-step docking procedure that first maximized the surface shape complementarity while minimizing the steric conflicts, but still with minor interpenetrations to implicitly account for some surface flexibility, and then allowed some explicit local side-chain flexibility to enhance the overall reliability. The candidate structures were then ranked by a binding score that includes energy contributions,

dipolar interactions and hydrogen bonds, as well as π-π and cation-π interactions. In this way, 121 proteins were sorted out as good targets for C_{60}, the best one being the voltage-gated K^+ channel that shall be described in more detail later. In most cases, as expected, the fullerene binding site was a hydrophobic pocket, in particular when the aromatic Trp, Phe and Tyr residues were present, but in many other cases a close interaction was also found with alkyl hydrophobic residues as well as with hydrophilic residues and with negatively charged Asp and with protonated Arg. It should be noted, however, that this approach cannot account for an induced fit interaction, because it does not allow for significant rearrangements of the protein. In any event, the interaction is expected to inactivate the protein functionality if the fullerene docking takes place in the active site, unlike the interaction with a hydrophobic pocket far from it. The same docking procedure was also adopted to investigate whether the proteins in the PDTD database do selectively interact with C_{60} or C_{70}, and whether they accommodate the fullerenes in the same or in a different hydrophobic pocket [9]. The two fullerenes have a slightly different size that also entails a slightly different curvature: these features can affect the interaction for steric reasons, but also the strength as an effect of topography. It turns out the even though a significant fraction of the chosen proteins do select C_{60} (about 17%), the majority of them (83%) does prefer interacting with C_{70}. Moreover most proteins (64%) accommodate the fullerenes in the same pocket, with very small differences in the location of their centers of mass (within less than 3.5 Å). This implies that these proteins can be used for fullerene extraction, the selected one being of course the fullerene yielding the most stable complex.

In Ref. [8] the docking procedure yielded as the first ranking protein the voltage gated K^+ channel, where C_{60} fit into the channel blocking it and hindering the ion movement, but actually both C_{60} and C_{70} were shown to fit in the same position [9]. Thus, the K^+ channel hosts the fullerenes in the hydrophobic cavity midway along the channel, but C_{70} is the preferred guest because it may show more interactions thanks to its larger surface. More recently, the C_{60} interaction within the K^+ channels was tackled by more extensive simulation methods that could afford a more detailed description of the involved factors from a structural and thermodynamic viewpoint [11•]. The docking approach was complemented by classical MD methods in water, while the potential of mean force was determined with the umbrella sampling method and molecular mechanics/Poisson-Boltzmann surface area (MM-PBSA) energy calculations were performed to estimate the free energy of binding. The latter method is often used to get this free energy through the potential energy contributions of the system and the free energy contributions to the solvation energy in implicit solvent. In this way, the possible blockage of the K^+ channel from the extracellular site was first considered, showing that binding to the entrance from this side corresponded to a local energy minimum higher than in the bulk solution: accordingly, it was concluded that only at large concentration C_{60} could block the channel from this side. On the other hand, when C_{60} approached the channel from the intracellular side, it could again weakly interact with the channel entrance, but eventually it could enter it with a strongly favorable energy and a rather large escape barrier of more than 20 kcal/mol. In conclusion, the fullerene blocks the channel by geometric factors, together with its hydrophobicity that allows for a significant binding interaction mainly with non polar residues, together with the release of the inner water molecules.

In contrast with the result for C_{60} enclosed within the K^+ channels, its interaction with lysozyme was not predicted by the docking approach of ref. [8]: this failure, at variance with experiments, was attribute to the use of pristine fullerene, whereas experimentally the observed complex with lysozyme was obtained with a fullerenol derivative, $C_{60}(OH)_x$ $x \approx 24$ [12]. However, since in the latter paper the interaction was attributed in particular to a π-π interaction with the aromatic system of Trp one expects that pristine fullerene should interact even more favorably, unlike what found by docking approaches. Indeed, the C_{60} interaction with lysozyme was experimentally found by NMR experiments which conclusively showed the existence of a 1:1 complex in water [13]. NMR and spectroscopic experiments, confirmed also by docking approaches, allowed identification of the highly specific binding pocket in the lysozyme catalytic site, and showed that the complexation does minimally affect the protein structure, with only a few residues being slightly perturbed. Spurred by this result, the interaction of pristine C_{60} with lysozyme was subsequently modelled more accurately using MD simulations and then analyzed through the MM-PBSA method [14•]. Starting with the experimental geometry, determined by the NMR experiments, the MD runs showed little changes in the complex geometry, but allowed calculating a favorable free energy of binding, dominated by the favorable van der Waals interaction with slightly unfavorable (i.e., destabilizing) solvation contribution and with some entropy loss (decrease of mobility of the amino-acid in the interaction site that belong to a random coil part of lysozyme.). The favorable interactions involved two Trp residues *via* π-π interactions and somehow more weakly the hydrophobic Ala and Val, but also some hydrophilic (Asn) and charged residues (Arg and Asp) partly thanks to their methylene groups. Interestingly, even though the polar or charged groups of the latter residues were still exposed to water, the proximity with C_{60} imposed some desolvation, whence a small but unfavorable solvation contribution.

Carbon nanotubes (CNT)

Protein can have the same effect as surfactants in solubilizing carbon nanotubes in a water environment, as first shown quite recently by MD simulations [15]. This paper was already reviewed in Ref. [7], and therefore we only report here the main findings for a comparison with more recent work. A comparison was made of the interactions of two protein subdomains comprising either α-helices or β-sheets with armchair CNT's having very different diameters both on the outer convex surface and on the inner concave surface. A strong adsorption was achieved in all cases, but on the convex surface the adsorption strength was found to increase with an increasing radius of curvature, being therefore largest on flat graphene. The opposite trend was observed on the concave surface, where the adsorption strength increased somewhat with a decreasing radius of curvature, provided this is small enough, i.e., provided the CNT diameter is significantly larger than the subdomain size. In the same paper it was also shown that oligopeptides with 16 residues could be easily encapsulated in CNT's with a smaller diameter of about 1.4 nm in a fully extended conformation, while such inclusion was limited to the terminal residues only with a smaller CNT with a diameter of 1.0 nm.

A more recent simulation study, supported by experimental results, does also suggest that a globular protein may also disaggregate large bundles of multi-walled CNT with a large diameter, but not the single-walled CNT with a small diameter [16••]. The chosen protein was a globular domain of C1q, a large multifunctional protein formed by six well separated globular domains, gC1q, each connected to a collagen stem that eventually form a single fibril. This protein can recognize bound antibodies in adaptive immunity, but it also plays an important role in various important processes. C1q appears to bind to CNT through its globular domains, and in this work this interaction is modeled considering a single gC1q domain to characterize it, resulting also in a study on the issue of CNT bundle disaggregation. MD simulations were carried out with an armchair (15, 15) CNT and more briefly a graphene sheet, evaluating also the free energy differences from the average forces. The plot of the free energy as a function of the distance from the center of mass of the carbon nanoparticle showed an attractive force towards gC1q and a larger change in the free energy at equilibrium that was much larger for graphene than for the CNT: this effect was attributed to the larger interacting surface of flat graphene compared to the curved CNT surface, allowing for a much larger footprint of the protein. An interesting finding was also that the Ca^{2+} ion sitting at the apex of gC1q far from the collagen stem was never close to the carbon surfaces: indeed, when it faced the carbon surface no adsorption was in practice observed. Thus, considering only a single globular subdomain does not appear to be a too significant simplification. The simulation results were also compared to experimental results reported in the same paper: the gC1q subdomain, separated enzymatically from C1q, was found to dissolve in water individual multi-walled CNT's with a diameter of ∼25 nm, but not single-walled CNT, which instead were solubilized as whole bundles. In order to explain this result, a theoretical model was proposed, showing that the interaction free energy per unit length among two CNT modeled as cylinders scaled as the square root of the tube diameter (see also [17]), whereas the adsorption energy per unit length of the nanotube scale scales as the square of the CNT diameter for relatively small CNT's, and linearly for larger nanotubes. Thus, below a certain critical radius, roughly calculated through estimates of the constants of these power-law dependences from the MD simulations, the lateral interaction among the nanotubes dominates at small nanotube diameter over the adsorption free energy, so that the small CNT remain bundled, where the opposite is true for larger nanotube diameters. Such conclusions are of great interest, but more extensive and detailed simulations must be carried out to confirm it, since for instance the structure of a multi-walled CNT with its nested nanotubes was not considered.

The effect of the surface curvature of CNT's, already investigated in Ref. [15] was later considered in more detail in Ref. [18]. In particular, the adsorption of bovine serum albumin (BSA) was modeled on four different armchair (n, m) CNT with $n = m = 15$, 20, 25 and 30 and the same number of C atoms, 3120, hence a progressively smaller length, together with a graphene sheet again with the same number of C atoms. Two different starting arrangements of BSA were considered, obtained by a 180° rotation of the protein. In all cases, a strong adsorption was found, confirming the earlier results [15] that adsorption becomes increasingly stronger on convex surfaces with an increasing radius of curvature. Thus, adsorption was increasingly stronger in the order (15, 15) CNT < (20, 20) CNT < (25, 25) CNT < (30, 30) CNT < graphene as measured through the number of heavy atom contacts, of the contact area and of the van der Waals interaction energy. The interacting regions of BSA were somewhat different on the different carbon surfaces, but in all cases they mainly involved hydrophobic patches containing in particular non polar and aromatic residues, as expected. On the other hand, the experimental results reported in the same paper did show exactly an opposite systematic trend. In order to explain this discrepancy, the authors noted that their simulations were carried out with single-walled CNT at a fixed mass, whereas the experimental data were obtained with multi-walled CNT at equal concentrations. In this case, an increasing diameter implies also an increase in the number of inner layers for the nested CNT's, so that the mass increases more rapidly than the

surface area. Therefore additional MD simulations were performed with multi-walled (20, 20) and (40, 40) CNT at a fixed number of atoms: because of this constraint, the former CNT had a much larger length and a larger external surface area than the latter one. For this reason, the adsorption eventually turned out to be stronger on the CNT with a smaller diameter, both in terms of the van der Waals interaction energy and the surface contact area. This result shows that the simulation and the experimental results should be carefully put in the proper context for a meaningful comparison.

The interaction of calmodulin with carbon nanomaterials was also investigated in order to assess how the adsorption on a hydrophobic surface can affect the dynamic properties of this protein [19,20]. Calmodulin (CaM) is a flexible messenger protein that regulates the calcium signaling pathways through rapid conformational changes, and is formed by two globular domains, each binding two Ca^{2+} ions, connected by a central α-helix. The interaction with a carbon nanomaterial may affect the dynamical properties of calmodulin upon adsorption, while they are crucial to its biological function. Accordingly, the interaction of calmodulin either in the presence of the Ca^{2+} ions (Holo-CaM) or in their absence (Apo-CaM) was modeled close to four armchair nanotubes, CNT (n, n) with n = 4, 5, 6 and 7 [19•]. It is found that the strong protein-CNT interaction affects the protein dynamics, which is no longer regulated by the cations, thus disrupting the protein function. The simulations compared the behavior of the isolated Holo-CaM with the experimentally determined geometry and of Apo-CaM, obtained by simply removing the metallic cations to that obtained for either system with each of the above-mentioned CNT, as well as the complexes formed with a 26-residue oligopeptide M13 as found in the structural data. The starting geometries were selected through docking procedures assuming a rigid protein structure, finding that only the two smaller CNT could sit in the CaM binding pocket, so that some local relaxation had to be imposed to CaM to host the larger CNT's. The MD runs (with a flexible protein) did not affect this arrangement, so that all the ligands (i.e., M13 and the CNT's) remained in the hydrophobic binding pocket, but increased the stability of the initial compact configuration of CaM. As for the ligand mobility within the binding pocket, it was found to be larger for M13 and CNT (6, 6), and conversely strongly constrained for the other CNT's. Therefore, all CNT favor a compact conformation of CaM, but the ligand mobility was affected somewhat differently. As for the interaction potential energy, it was largest for M13 thanks to the presence of intermolecular H-bonds, in addition to the hydrophobic interactions, but for each ligand the interactions of Apo-CaM were weaker than those with Holo-Cam for M13 and CNT (4, 4), whereas the differences are of the opposite sign but much less significant with the other CNT. In conclusion, these simulations indicate that with M13 the Ca^{2+} coordination is crucial for the ligand binding and the CaM compactness, and a similar mechanism may be present with the smaller CNT (4,4). On the other hand, with larger nanotubes the Ca^{2+}-regulated binding mechanism is less effective, so that the protein functionality may effectively be disrupted.

Graphene and graphyne

Calmodulin both with and without its four Ca^{2+} ions (Holo-CaM and Apo-CaM, respectively) was also used to test the behavior of graphyne nanosheets [20]. Adopting two starting orientations rotated by 180°, at the end of the MD runs it was found that the adsorption of Holo-Cam was favored over that of Apo-CaM if the graphyne plane was approached proximal to the inter-domain linker, whereas they showed the same adsorption strength when approached distal to it. Adsorption was facilitated by bending of the inter-domain linker, driven by strong hydrophobic interactions, but both globular domains did interact with the graphyne sheet only in the distal system. While in the isolated state the Holo form shows smaller deviations from the original geometry than the Apo form, probably thanks to the presence of the Ca^{2+} ions, on graphyne the Holo form showed again small changes independently on the starting orientation. On the other hand, the Apo form showed somewhat larger changes than Holo, but a contact surface area and an interaction energy much affected by the starting arrangement. Analysis of these quantities shows that the proximal Apo-CaM binds less favorably than the Holo-CaM, indicating that a large hydrophobic region on the proximal side of the linker is only exposed in the presence of the Ca^{2+} ions (Holo form), but remains hidden in the Apo form. Also, the interaction strength of the Holo form in the proximal adsorption implies that a strong interaction is required to desorb it and separate the complex. Overall, graphyne appears to interfere with the CaM by affecting the geometry of the two globular domains and disrupting the Ca^{2+} signaling pathway. The presence of a graphyne quantum dot inside the CaM binding pocket was also modeled through a small molecule formed by a lozenge having four aromatic rings at its vertices, the sides and the short diagonal comprising a −C≡C- group each in order to mimic a binding ligand. The results show that this ligand is well docked in the hydrophobic pocket both for the Holo and the Apo forms, but with smaller protein changes in the former case, showing again that the Ca^{2+} ions do conformationally stabilize CaM, even though the contact area and the interaction energy with the quantum dot are independent from their presence.

A very interesting paper has also analyzed in detail the great relevance of charged basic residues (Arg and Lys) in addition to the hydrophobic interactions for protein adsorption on graphene [21••], and more generally also on other pristine carbon nanomaterials, as already

previously found but non clearly stressed or possibly even noticed (see for instance Refs. [8,14,15]). The coating of a graphene sheet by proteins, forming the so-called protein corona, may reduce its cytotoxicity [22] and accordingly simulation studies have been undertaken to model such coating by blood proteins. The present paper [21] considered bovine fibrinogen (BFG), and then more briefly BSA as important examples. BFG is a hexamer with two homologous halves linked by disulfide bridges, and each half is formed by three long intertwining α-helices and a terminal β-sheet domain. Considering two starting orientations having the helical axis parallel to graphene, three independent runs were carried out. The simulations yielded an increase of the number of atoms in contact with the surface, together with an increase of the contact surface area. On the other hand, the conformational changes with respect to the crystal structure were relatively modest, involving only a few stepwise local loosening of some helical turns enhancing the contact between specific residues and the surface. These residues were the aromatic amino-acid (Trp, Tyr and Phe), but also the basic protonated Arg and Lys. The interaction energies of these individual residues were quite similar, and indeed in certain strands of the three helices the basic residues were more tightly bound to the surface than the aromatic ones. A detailed analysis showed that this observation is related to the planar nature for instance of the protonated terminal group in Arg, but also to the fact that in spite of adsorption the hydration of the charged groups underwent a minor decrease, compensated or even offset by the favorable hydrophobic interaction of the connecting alkyl chain. In this way, the overall interaction was at least as favorable as that due to the π-π stacking of the aromatic residues with the graphene surface. Similar results were also found for BSA on graphene. It should be pointed out that essentially the same results were also found in the MD simulation of selected tripeptides on graphene [23]. The tripeptides had the general structure Gly-X-Gly, X being one of the twenty natural aminoacids: the calculated binding enthalpies showed again that the most favorable absorption was due to the basic residues with X = Arg or Lys, followed by hydrophilic neutral Asn and Gln, and then by the aromatic Trp. Furthermore, advanced quantum chemical DFT calculations have also shown the same trend in the interaction strength of individual residues on a fullerene and on a CNT surface, as reviewed in detail in Ref. [7], in spite of the known limitations of DFT to accurately account for the dispersive energy contributions.

In view of these considerations and results, it is quite surprising that the above-mentioned simulation results stressing the role of basic residues [21] were not considered or found again in a contemporary paper by the same group dealing with the adsorption of graphene of the same BFG and BSA proteins, as well as of immunoglobulin (Ig) and transferrin (Tf) [24]. The aim of this paper was to compare the graphene adsorption of these four proteins that may reduce its cytotoxicity by forming a corona endowing it with a new biological identity. The simulation results were compared with experiments, which however were carried out on graphene oxide (GO) and on reduced GO (rGO): even though large non-oxidized regions can be present on GO and in particular on rGO, where the oxygen content was about 3% only, simulations on a real GO surface would be of interest (see later, however). On pristine graphene, according to these simulations the BFG adsorption was driven by hydrophobic interactions only, involving the π-π stacking of Trp, Tyr and Phe with graphene, indicating some protein unfolding (helical deformations) that exposes to the surface some buried hydrophobic residues. The simulations of BSA showed similar interactions involving in particular the aromatic and the hydrophobic residues, with a concomitant expulsion of water molecules from the protein-graphene interface. More generally, the interactions energies of the four modeled proteins were roughly correlated with their molecular weight and hydrophobicity, as well as with the contact number of aromatic residues, but the relative weight of these contributions was not assessed. On the other hand, no mention was made of the relevance of the charged basic residues, and actually no interactions between them and graphene was found, in particular in the case of BFG, at variance with the results found in Ref. [21] for the same protein. This issue is quite puzzling, and certainly requires further simulations to be clarified.

A different issue was tackled in another simulation study of a fragment of viral protein R (VpR) comprising 21 helical residues adsorbed on graphene [25•]. In this way, the authors could model possible conformational changes of this α-helical fragment to an antiparallel β-sheet structure induced by graphene, as experimentally found on GO [26], thus suggesting a stiffer structure of the latter motif. In this case, the fragment was quickly adsorbed on the surface and then slowly rearranged itself with relatively modest changes in the contact surface area in order to maximize the number of contact atoms and the interactions among the residues, in particular through their side groups. Interestingly, the residues most responsible for a strong interaction through van der Waals energy were the aromatic Tyr and Trp residues, but also the basic ones, namely Arg and Lys, in keeping with the results reported in Ref. [21]. As for the conformational changes, analysis of the trajectories through the Ramachandran plot revealed a significant fraction of β-sheet structure: however, this structure, involving only a few residues, was reversibly formed and destroyed during the simulations, and did not propagate. Most probably, longer strands and possible multiple oligopeptides are required to stabilize the β-sheet structure through more inter-strand hydrogen bonds.

Another issue, related with the problem of the potential toxicity of graphene, was taken into account by modeling the interaction of three proteins having different secondary structures, namely, α-helices, β-sheets or their combination, assuming that conformational changes and denaturation could lead to loss of functionality, hence to toxicity [27]. Unfortunately, the protein sizes were quite different, comprising only 28 residues for the protein with a α-helix and a β-sheet, 40 residues for the β-sheet domain and 80 residues with α-helices only, so that possible molecular weight effects could not be assessed. The simulations adopted classical MD simulations in water, while the MM/GBSA method was used for the free energy calculations in implicit solvent. In all cases, adsorption was found to be a fast process that in some cases required lengthier stepwise rearrangements to maximize the number of atoms in contact with the surface with a significant surface spreading. The driving force for adsorption was only due to hydrophobic interactions, and the interaction was most favorable for the α-helix than for the β-sheet. We believe that this finding may be related to the different protein size, but also to the different rearrangements close to the surface that may destroy the secondary structure. Anyway, the MD simulations indicated that the α-helix structure in the larger protein was mostly destroyed, even though the amount of denaturation was also related with the starting orientation which affected the initial contact, while the triple-stranded β-sheet was found to be more robust. Interestingly, in the smallest protein the α-helix and the β-sheet secondary structures were largely destroyed, but again this could be a consequence of the small molecular size. It should also be added that adsorption was mainly attributed to the interaction of hydrophobic residues, and in particular to the aromatic ones, but still the hydrophilic ones provided a significant contribution to the favorable van der Waals interaction energy, thanks also to their large number.

We would like to end this paragraph by noting a recent paper that modeled the adsorption of a helical oligopeptide comprising 16 natural aminoacids with a chiral C_α adsorbed on two enantiomeric chiral CNT [28•]. Chiral CNT are characterized by (n, m) indices with $n \neq m$: in chemical terms, enantiomeric chiral nanotubes have swapped indices (n, m) and (m, n), and can interact with chiral molecules such as the oligopeptides forming in principle complexes with an unlike stability. The selected CNT were the (10, 20) and the (20, 10) CNT with a diameter of 2.07 nm, while an armchair (16, 16) CNT with a very similar diameter was also considered for a comparison. The MD simulations, carried out in an implicit solvent, considered four starting oligopeptide orientations close the outer CNT convex surface, and other four ones close to the CNT open end, but outside the inner cavity, to model adsorption on the concave surface if encapsulation took place in the MD run. Adsorption was eventually achieved both on the outer and on the inner CNT surface, the latter concave surface producing a stronger adsorption than the former convex one in all cases. Most interestingly, however, it was found that both on the inner and on the outer surface the selected oligopeptide showed a significantly stronger adsorption on the (20, 10) CNT than on the enantiomeric (10, 20) CNT, with the armchair (16, 16) CNT being somewhat in between. In particular, adsorption on the inner surface had roughly the same strength on the (10, 20) and on the armchair (16, 16) CNT, but weaker than on the (20, 10) CNT, while adsorption on the outer surface of the (20, 10) CNT was about as strong as that on the armchair (16, 16) CNT, and anyway stronger than on the (10, 20) CNT. The interaction energy was dominated by the van der Waals interactions of the hydrophobic Ile and Leu residues and by the π stacking interactions of the aromatic residues with the CNT surface, while a few hydrogen bonds among the oligopeptide side groups provided a further oligopeptide stabilization. The conclusion of this study was that suitable oligopeptides of a sufficient length could be used for the chiral separation of enantiomeric CNT's, and vice versa that molecular sieve membranes with aligned chiral CNT with a single handedness might act as chiral selectors for racemic mixtures of synthetic oligopeptides.

Oligopeptide insertion into carbon nanotubes

As mentioned in the Introduction, CNT can be used as drug delivery systems. For instance, they can be surface coated with antimicrobial peptides (AMP) to generate antimicrobial surfaces, thus possibly allowing for their solubilization in water. MD simulations recently modeled the interaction with carbon nanomaterials of an AMP comprising 20 residues, CA−MA, obtained as a hybrid of Cercopin A (CA) with 37 residues and Magainin 2 (MA) with 23 residues [29]. The CA−MA hybrid was found to have better antimicrobial and antitumor activities compared to the individual AMP's, and therefore could be used to prevent bacterial contamination of drug-delivery systems based on CNT's. The interaction of CA−MA molecules was thus modeled on an armchair (10, 10) CNT and a graphene sheet having the same surface area, adopting for the peripheral carbons a united atom model mimicking a C−H group. Additional simulations included an explicitly hydrogenated and a fluorinated CNT obtained by capping the terminal C atoms with explicit H atoms and with electronegative F atoms. Considering the simultaneous presence of four CA−MA molecules, the MD simulations indicated adsorption on both sides of graphene, with three randomly arranged molecules on one side of the graphene sheet, and the fourth on the other side after migration, most likely for the lack of space. A relatively similar result was obtained on the CNT, but in this case three CA−MA molecules were fully spread on the outer surface, while the fourth one

was encapsulated almost completely inside the CNT, a behavior strongly similar to that reported in Ref. [15]. Also in this case, on the π-π interactions were optimized, while the polar residues protruded towards the bulk solvent. It is interesting to monitor the diffusion of one CA−MA molecule inside the CNT: the rate determining step of this process is the search of the appropriate orientation of a terminal neutral residue in order to enter the nanotube, thus being largely entropic, since after insertion the diffusion of the molecule inside the cavity is relatively fast. In order to better understand this encapsulation process, a further simulation was also performed for a single CA−MA molecule placed close to the entrance of a CNT capped with explicit hydrogens or fluorine atoms. Interestingly, encapsulation was achieved with the united atoms at the CNT rim and with the fluorinated rim, but not with the hydrogenated rim. Rather, in the latter case the CA−MA molecule was adsorbed on the outer surface. The authors explain this behavior with electrostatic effects due to the positive charges on the peptide which favorably interact with the partial negative charges of the fluorine atoms, but are repelled by the H atoms having a slightly positive charge. However, in view of the very small charge of the hydrogens (+0.1), we feel that the issue requires further studies and simulations: for instance, many independent runs should be attempted so as to test for instance the effect of the random initial velocity, thus getting also an estimate of the probability for insertion.

Functionalized carbon nanomaterials

A huge interest about the nanomedicine relevance of fullerenes was spurred by the report in 1993 that fullerenes can inhibit the HIV-1 protease by binding to the active site [30]. Actually, while in this paper the theoretical results, obtained through docking calculations, were carried out with the pristine hydrophobic fullerenes, the experiments were carried out with functionalized, water-soluble fullerenes. The inhibitory effect on HIV-1 protease was also obtained by the screening procedure of ref. [8], but again only the pristine C_{60} fullerene was considered. Therefore, the functionalized fullerenes interaction with HIV-1 protease was modeled more recently considering C_{60} derivatives with various polar substituents tuning their hydrophilic behavior [31]. In this paper, 49 fullerene derivatives were considered that mostly contained substituents carrying oxygen atoms in hydroxyl, carboxylic or ethereal groups, or nitrogen atoms as amine groups, and their combination in amide moieties, while in other derivatives a few substituents were fully hydrophobic alkyl and aromatic groups or fluorinated aromatic moieties. The geometry of these derivatives was fully optimized by state-of-the-art quantum mechanical DFT methods, and then a docking procedure was applied using a protein geometry optimized by classical molecular mechanics methods. The docking was performed considering a rigid receptor (the protein) and a flexible ligand in view of the possible flexibility of the fullerene substituents, and quantitative structure−activity relationship (QSAR) approaches were then used using molecular descriptors obtained for the receptor through DFT methods, and for the ligand through structure-based additive descriptors to predict the binding affinity. The docking analysis suggested that the fullerene derivatives were located into the hydrophobic pocket, forming a few hydrogen bonds with the surrounding aminoacids, and suggesting that the polarity of the C_{60} substituents had only a minor effect on the ligand−protein interaction. In this way, it was possible to show that the feature affecting the activity of the fullerene derivatives were related to the molecular geometry, the number of rings of the substituents and the molecular topology., with the aromatic rings enhancing the intermolecular interactions through π-π stacking.

More recently, the screening approach originally proposed in Ref. [8] was adopted to model the interaction of the PDTD proteins [10] with 169 functionalized fullerenes decorated with various small moieties in addition to non-functionalized C_{60}, C_{70} and C_{80} [32•]. The procedure comprised both docking and cheminformatics methods, but also some MD simulations in a few interesting cases. In this way, the behavior of the hydrophobic fullerene modulated by the presence hydrophilic substituents could be assessed with the aim of screening for either drugs targeting specific proteins, or for potentially toxic molecules. First of all, the functionalized fullerenes were grouped in six main clusters based on their similarity: the first and the largest cluster comprised six-membered rings with one or two double bond, the second one aliphatic rings, the third one aromatic rings, all being variously substituted with branched substituents. The other clusters comprised mainly oxygen-containing substituents, or mostly nitrogen carrying groups, or else with substituted smaller rings (cyclopropane and cyclobutane). Protein docking was then applied to find which fullerene derivatives could be considered as toxic being non specific in binding, since they efficiently bound to more than 50% of the tested proteins, and those that were highly selective, thus potentially being good drugs or drug delivery systems. Afterwards, the best ligand was identified for each protein, discarding the fullerene derivatives interacting with the protein surface since they could not be docked in the active site. This docking procedure allowed recognizing 26 top ranking fullerenes derivatives interacting with 11 proteins, subjected to a more detailed energy interaction analysis, thus revealing also which part of the ligand mainly contributed to docking. In all cases, the driving force for interaction was found to be due to hydrophobic interactions, whereas hydrogen bonds played a minor role or even decreased the binding. Four among the best ranking protein-ligand system was the subjected to MD

simulations in water: the complexes turned out to be quite stable, even though some local reorganization could sometimes take place. In any case, no large displacement of the residues appeared to be present, thus supporting the results of the adopted docking procedure. In conclusion, the study showed that computational techniques can be very efficient to assess the potential toxicity of fullerene derivatives through their non-selective binding, and to sort out the potential drugs through their selectivity.

Experimentally, fullerenes are often functionalized with polar groups such as hydroxyl and amino groups in order to improve their water solubility. Accordingly, in the last few years the interaction of these functionalized fullerenes with proteins has also been considered. For instance, the interaction of a model protein, ubiquitin, with fullerenols carrying various numbers of OH groups bound to C_{60} was modeled using both docking methods and MD simulations [33] in comparison with experimental results obtained with $C_{60}(OH)_{20}$. Ubiquitin is very diffuse, being present in most tissues of eukaryotic organisms, and was chosen because of its relatively small size. The hydroxylated fullerenes had the general formula $C_{60}(OH)_x$, with $x = 0, 4, 8, 12, 16, 20$, where the first case is the pristine fullerene, whereas the latter one ($x \approx 20$) corresponds to the experimentally used fullerenol. The docking simulations considered many trials assuming a rigid protein and fullerenes, and allowed selecting the most favorable binding sites. Subsequent MD runs were carried out with randomly placed the $C_{60}(OH)_{20}$ fullerenol molecules around ubiquitin, which allowed testing for the different interaction sites in a single MD run. The MD simulations adopted two methodologies: the first one employed classical atomistic simulations in explicit water, and in the second one an implicit solvent was chosen using Discrete Molecular Dynamics (DMD) methods with implicit solvent [33], which allows probing much lengthier time scales although possibly neglecting relevant hydration effects. The driving force for the protein-fullerenol interaction was again fount to be based on the hydrophobic interactions, involving in particular the π-π stacking interactions, so that an increasingly larger number of hydroxyl groups leads to weaker interactions, hence to a lower binding affinity. As a conclusion, it was suggested that a limited number of hydroxyl groups on the fullerene molecule do induce larger protein misfolding upon penetration in the hydrophobic core.

Most recently, the binding of pristine C_{60} and of its water-soluble derivatives $C_{60}(NH_2)_{30}$ and $C_{60}(OH)_{30}$ to tyrosine phosphatase was modeled through docking approaches and extensive MD simulations [34]. This protein contains two close domains (labelled as D1 and D2) that show complementary surfaces and interactions, thus maintaining the relative orientation and the protein stability. The simulations showed that the three fullerenes can sit within the region between D1 and D2 separating them to some extent, destroying the native structure even upon small changes, the largest effect being shown by $C_{60}(NH_2)_{30}$. The optimized fullerenes geometries were initially docked between the protein using the procedure proposed in Ref. [8] and also adopted for instance in Ref. [31]. The complexes obtained for the three fullerenes with the highest score were then subjected to MD runs in explicit water. The docking simulations showed that all the fullerenes were found in the region comprised between the D1 and the D2 region, and the MD simulations displayed little changes in the geometry of the three fullerenes bound to the protein, whereas the protein showed larger changes, but still less than in the free state. Interestingly, only very few hydrogen bonds were formed between the functionalized fullerenes, and less for $C_{60}(OH)_{30}$ than for $C_{60}(NH_2)_{30}$, and therefore the largest interaction was found for the pristine fullerene thanks to the much larger hydrophobic van der Waals interaction, while $C_{60}(NH_2)_{30}$ and $C_{60}(OH)_{30}$ showed progressively weaker interactions. From the viewpoint of the protein conformation, however, these interactions have far reaching consequences in the mutual orientation of the D1 and D2 domains, because C_{60}, fully inserted between the two domains, may pull them closer to one another with a slight tilt in their orientation. Conversely, $C_{60}(NH_2)_{30}$ and $C_{60}(OH)_{30}$ were located on the same region at the periphery of the two domain, producing a larger tilting of the two domains, in particulary for the amino derivative, with a different hydrogen bond pattern between the two domains compared to the isolated protein. Additionally, significant conformational changes were found in the D1 domain, containing less secondary structure than D2, richer in α-helices. These conformational changes in the active site of the protein can thus explain the inhibitor effect of fullerenes on tyrosine phosphatase.

Modeling the protein interaction with functionalized CNT's through MD simulations received less attention compared to substituted fullerenes and graphenes. The behavior of single-walled CNT functionalized with prolines or arginines and interacting with the Src homology 3 (SH3) protein domain that mediates protein–protein interactions, was recently investigated [35]. This protein binds with high specificity to Pro and other hydrophobic aminoacids, such as the proline-rich motif PRM, an octameric oligopeptide containing four Pro, a Val and two terminal Arg. PRM binds to SH3 by first anchoring with the Arg residues to negative patches of the protein, and then binding the other residues in the hydrophobic pocket. An earlier work by the same group [36] had shown that pristine armchair (3, 3) CNT, selected for a good fit in this pocket, has a stronger binding affinity than PRM thanks to its strong hydrophobicity though lacking positively charged groups. Therefore, it inhibits the PRM regular binding,

suggesting potential CNT toxicity. In the more recent study [35], the same CNT was modeled considering its functionalization with *i*) three bound Pro (P3-CNT), *ii*) one Arg (A1-CNT), *iii*) two linked Arg (A2*l*-CNT) or *iv*) two separate Arg (A2*s*-CNT). The MD simulations (replicated 10 times for each case) clearly showed quite surprisingly that the functionalization did not improve significantly or even reduced the specificity of the CNT-SH3 interaction. Thus, the P3-CNT system was only slightly more specific than CNT for steric reasons in four out of the 10 simulation runs, because when the prolines were inside the binding pocket, the CNT could not make efficient contacts due to its rigidity (unlike the flexible PRM). As for A1-CNT, the single arginine allowed for long-range recognition, with a modest improvement of the SH3 recognition over the bare CNT, whereas with A2*l*-CNT the binding success surprisingly dropped, being only achieved in three runs: in fact, a clamping mechanism around a negative patch firmly kept blocked the functionalized CNT for quite a long time before the two Arg could make contact with two different patches in the successful runs. Also in the case of the A2*s*-CNT system the two separated Arg, linked however to one CNT end in close proximity, showed the same clamping mechanism, leading to successful binding only in one run out of ten. Interestingly, this clamping mechanism was also found in the control simulation of PRM with the SH3 domain in three out of ten runs, but the oligopeptide flexibility could curl itself allowing the Pro to find the binding pocket. In conclusion, it was stressed that the nanomaterial functionalization presents many inherent subtle feature that require a careful control of the various factors and their interplay.

Experimentally, carbon nanotubes are usually functionalized either non-covalently through amphiphilic molecules that can interact with the hydrophobic CNT's while solubilizing them through their polar groups, or covalently upon chemical reaction with polar, water soluble groups. Clearly, the presence of these groups at the CNT surface can also affect the interaction with proteins. One example of such a system was recently modeled by molecular dynamics simulations considering an armchair (15, 15) CNT with a diameter of 2.03 nm [37•]. This CNT was non-covalently functionalized with a surfactant, sodium hexadecyl sulfate (SHS) able to solubilize it in water: the MD simulations showed that the long hexadecyl chains fully wrapped the CNT, while the sulphate heads, vertically oriented away from the carbon surface, were exposed to water. Next, the interaction of lysozyme with the SHS-CNT system was modeled, and compared with a lysozyme-CNT control system, where a CNT diameter of 4.0 nm, possibly to achieve the same exposed surface area and the same curvature. Different starting orientations were considered, and the most favorable one eventually yielded the final protein arrangement. Adsorption was found to be due to enthalpy effects, with some increase of the water entropy initially solvating the functionalized CNT. Quite small conformational changes were found for the bound protein compared to the isolated one, in keeping with the CD spectra, whereas the SHS molecules underwent significant rearrangements, forming a saddle-like structure well fitting the lysozyme shape thanks to the electrostatic interactions among them. A main result however is that the cleft of the active site was exposed to water, thus preserving the biological activity. Conversely, on the bare CNT the active site was found to interact with the CNT surface, since most of its residues are hydrophobic, therefore showing a lower activity than in the former case.

The typical functionalizations of graphene is achieved by oxidation that forms graphene oxide (or GO) containing epoxy and hydroxyl groups together with carboxylate groups often assumed to be confined to the nanosheet edges. In this way, the GO surface becomes hydrophilic and water-soluble; another experimentally used is the moderately hydrophobic reduced GO (or rGO), where the oxygen content is strongly decreased to a few percent. The effect of graphene functionalization on protein adsorption was quite recently studied through MD simulations of a long α-helix containing 41 residues taken from the complexin protein interacting with a graphene, rGO (having a C:O ratio of 20:1) or GO surface (with a C:O ratio of 5:1) [38]. Unfortunately, the size of the nanomaterial surface closely matched the helical length, so that edge effects were most likely present, and furthermore the simulation length was not sufficient to achieve an equilibrium state in all the MD runs. Anyway, in all cases the α-helix was adsorbed on the nanomaterial surfaces, while the number of atoms in contact with it was roughly the same, being however slightly larger on graphene than on rGO and somewhat smaller on GO. On the other hand, significant conformational changes were only detected on pristine graphene with a large disruption of the helix, whereas minor loss of the secondary structure was achieved on rGO and on GO. It was also pointed out incidentally that the helical denaturation on the most hydrophobic surface entropically favored the helix adsorption, in addition to the enthalpic favorable contribution. Interestingly, the interaction energy was basically the same on the three surfaces, but different contributions were present: on graphene, only the van der Waals interactions were clearly present, whereas an electrostatic contribution was also present on rGO and in particular on GO. The latter contributions were found to be due to the interaction of the charged basic residues Arg and Lys, often hydrogen bonded to the surface oxygen atoms, and of the neutral Tyr, while no π-π stacking was essentially found.

A subsequent study modeled the interaction of α-chymotrypsin (ChT) with pristine graphene and with

GO to understand the very large inhibitor effect shown by the latter surface on the activity of the ChT enzyme [39•]. In this case, the GO surface comprised one epoxy oxygen and one OH group every 10 C atoms and one carboxyl group every 20 C atoms at the nanosheet edge. Three random orientations were selected for each surface, having anyway the active pocket facing away from it. A proflavine molecule was eventually docked to the active site at the end of the MD runs to monitor the change of activity of the adsorbed ChT. On graphene the hydrophobic Ile, Val, Ala, Pro residues mostly contributed to the interaction, together with one Phe showing a π-stacking interaction with the surface, but also one Arg residue was involved, though to a lesser extent and with its alkyl chain not in contact with the surface. The α-helix was not involved in adsorption, unlike what found on GO where most residues interacting with the surface were the hydrophilic Lys and Asn that formed many hydrogen bonds with the surface oxygens. The different interaction pattern on the two surfaces is such that the active binding pocket is always far from the surface when adsorption took place on graphene, so that the biological activity is essentially unaffected. Conversely, on GO it is adsorbed on the surface and is significantly affected, being in practice squeezed to a much smaller volume. These observations were also further confirmed by the proflavine docking results. Therefore, the simulations agree with the observed inhibitory effect of GO on α-chymotrypsin, suggesting also that a strongly different behavior would be observed on pristine graphene, while inhibition could also be modulated by tuning the surface properties.

Finally, a most recent paper described an analogous adsorption of cytochrome *c* (Cyt *c*) on pristine graphene and on GO [40] having the same fraction of oxygen atoms as in the above-mentioned paper [39]. The secondary structure of this protein consists of five α-helices and two short antiparallel β-sheets, and a porphyrin ring (a heme group) is present with a central ferric ion which can lead to electron transfer with graphene-like materials. The simulations adopted a preliminary parallel tempered Monte Carlo (MC) simulation in order to find the preferred initial orientation on the surface to be used in subsequent MD runs. In the MC simulation, the protein was simply described through its C_α atoms and was kept rigid, while a structureless surface was employed having van der Waals and (for GO) electrostatic interactions with the positively charged protein into an implicit solvent. The preferred conformations thus achieved were subjected to long MD runs, yielding different final orientations on the two surfaces: Cyt *c* showed the heme group close to and roughly perpendicular to the negative GO surface, while the same group was far from the neutral graphene surface, and tilted with respect to it. Therefore, on the latter surface there can be no effective electron transfer simply because of the large distance between the iron cation and the surface, whereas the smaller distance on GO allows for a quite efficient electron tunneling. The adsorption leading to this different behavior was in fact due to the different interactions, so that on GO the number of atoms in contact with the surface is larger than on graphene, but in particular the interaction energy is much larger (in absolute value), being dominated by the electrostatic forces between the negatively charged groups on GO and the positively charged residues in Cyt *c*. The strongest interactions on GO were shown by the Lys residues bound with hydrogen bonds to the surface oxygens (shown also by Gln), and on graphene mainly by the aromatic Tyr by the oppositely charged Lys and Asp, closely followed by both polar and non-polar residues such as Asn, Ile and Pro. The relevance of polar residues to achieve strong interactions with graphene, while still being quite well solvated, is thus confirmed [21].

Carbon nanomaterials and oligopeptide or protein aggregates

Several neurological disorders involved in the Alzheimer's and the Parkinson's disease are today related with the association of amyloid-β peptides (Aβ-peptides) into fibrillar aggregates formed by extended β-sheets. CNT have been shown to interact with the fibrillation process by either retarding or promoting it depending on the involved peptides. Therefore, much simulation effort was recently carried out to model this interaction between carbon nanoparticles and short oligopeptides able to form fibrillar β-sheet aggregates. In particular, Wei et al. first modeled the interaction of the amyloid β (Aβ) sequence of eleven aminoacids Aβ 25−35 with single-walled armchair CNT having a slightly different size (i.e., (4,4) and (5,5) CNT) in water [41]. The starting geometry involved two antiparallel β-sheets containing a total of eight oligopeptides (an octamer), and then a decamer, forming two planar sheets that were positioned in water or parallel to the CNT axis. While the isolated strands did evolve into a random aggregate, the hydrophobic aggregates yielded a structured β-barrels around the CNT with a concomitant dehydration of the interface. Therefore, these simulations suggest that carbon nanotubes may enhance the fibril formation of the Aβ 25−35 oligopeptides that would otherwise form random aggregates. On the other hand, an analogous simulation approach [42] suggested that the same CNT inhibited the formation of β-sheet oligomeric structures with the closely related octamer formed by the oligopeptide with seven residues Aβ(16−22) with a hydrophobic core. In this case, the starting arrangement of the oligopeptides was irrelevant, since the same results were obtained both from an amorphous arrangement, and from a preformed β-sheet octamer having the β-barrel structure formed in solution by an MD simulations. It should be noted that Aβ(16−22) is a zwitterionic oligopeptide comprising near the chain ends both a positive charge on a Lys residue and a negative charge on

a Glu residue, together with both alkyl and, in particular, aromatic hydrophobic residues. An important result of this study is that carbon nanotubes do favorably interact with the oligopeptides, but strongly inhibit the β-sheet structure formation in Aβ(16−22), unlike what was found for Aβ 25−35 [41]. Unfortunately, the authors did not analyze in much detail the reason for this different behavior, but still stressed the relevance of the π-π stacking interactions of the Phe residues with CNT for the former oligopeptide.

The issue of the fibril formation by the octameric Aβ(16−22) in the presence of fullerenes of different sizes [43] and of hydroxylated CNT [44] was also investigated more recently by the same group. The first of these papers dealt with the effect of pristine carbon nanoparticles of different sizes and concentrations, namely an individual C_{60}, three such molecules, $3C_{60}$, and the larger fullerene C_{180}, with the same number of C atoms, but obviously a smaller surface area [43]. The replica-exchange MD simulations (REMD) in water carried out at different temperatures allowed probing more efficiently the configurational space of the modeled systems, thus improving the ergodicity of the simulation. In the presence of a single C_{60}, the Aβ(16−22) octamer displayed the same aggregation behavior in antiparallel β-sheets as the isolated system, indicated that *per se* the oligopeptide aggregation was not affected by the presence of C_{60} in the 1:8 ratio. Conversely, in the larger 3:8 ratio, i.e., for the octamer in the presence of $3C_{60}$, the β-sheet formation was inhibited in terms both of their formation probability, and of their size. Quite surprisingly, the larger C_{180} fullerene had an even larger inhibitory effect in spite of its smaller surface area compared to $3C_{60}$, increasing the population of disordered aggregates. This effect was attributed to the larger number of six-membered rings in the larger fullerene compared to that in $3C_{60}$, which favored the π stacking interactions of the nanoparticle with Phe. However, the effect of the smaller surface curvature in C_{180} could also play a significant role, since it favors the intermolecular π-π interactions, a feature not fully considered in the quoted paper [43].

A similar inhibitory effect on the aggregation of the same octameric Aβ(16−22) was also displayed by a hydroxyl-functionalized CNT. In particular, a single-walled CNT with 216 carbon atoms was considered with 30 uniformly distributed OH groups covalently bound to its surface [44]. Unfortunately, no detail was provided for the CNT structure, apart from its diameter, amounting to 0.407 nm. Also in this case, it was found that this functionalized CNT did prevent the formation of β-sheets both in terms of a lower probability of formation, and of their smaller size, producing instead coil-rich aggregates. In this case, the culprit responsible for the lack of structured aggregates was found to be the presence of many hydrogen bonds between the CNT and the oligopeptides inhibiting the formation of similar interactions among the latter ones and therefore decreasing the interaction energy among the individual oligopeptides.

In a different area, the interaction of pristine graphene and graphyne on the dimeric, non-covalent association of proteins was also modeled to understand the potential nanotoxicity of these materials when they affect the protein−protein interactions having a hydrophobic interface. One example of such system interacting with graphene is the C-terminal DNA binding domain of human immunovirus-1 integrase [45•]. This protein is dimeric in solution, each monomer containing a five-stranded β-barrel structure and the barrel axes roughly orthogonal to one another. The monomers interact through a hydrophobic interface thanks to six residues comprising Leu, Trp, Ala Val and Ile. Therefore, the dimer separation through graphene intercalation may lead to potential toxicity of this nanomaterial. MD simulations of the isolated dimer in solution showed its conformational stability, showing a nearly unchanged intra- and inter-molecular geometry compared to the crystal structure. The MD simulations with graphene were carried out starting with the sheet parallel to the dimer interface, but at opposite sides, so that in one case it could interact with the hydrophobic sides of the monomers, and two independent runs were carried out for each starting geometries. In either case, the final result was that graphene did insert within the hydrophobic interface, separating the two monomers, so that eventually they were adsorbed on opposite sides of the graphene nanosheet. Two different mechanisms were found: the graphene nanosheet could directly insert very quickly between the two monomers if placed close to the hydrophobic side of the dimers, otherwise a more lengthy pathway could be adopted, whereby the graphene nanosheet may somehow interact with the side of one monomer before entering the interface. The hydrophobic interactions among the protein interfaces and graphene were the driving forces to separate the protein monomers and to allow the nanosheet insertion within the interface. Anyway, this insertion allowed to minimize the unfavorable interactions of graphene with water and to maximize the hydrophobic or van der Waals interactions with the protein monomers. As further points of interest, the authors stressed two points. On one hand, the two protein monomers basically kept their original conformations, but the barrel axes assumed a parallel orientation of their main axes, which may hint to some inter-barrel interactions that may be present through the graphene sheet: interestingly, this issue was not addressed explicitly, but we point out that in this adsorption geometry weak non-bonded interactions between the intercalated proteins may still affect their adsorption geometry. On the other hand, the atomically flat graphene allows for a larger contact area with either protein monomer, whence a stronger interaction

compared to that present with the rougher protein envelope.

The same protein dimer was also modeled in the interaction with a graphyne nanosheet following the same procedure [46]. The simulation results showed again that graphyne could interfere with the protein–protein interface, separating the dimer by insertion in the hydrophobic interface between the dimer. However, adopting the same simulation protocol previously followed for graphene, it was found that even starting from the hydrophobic site of the protein dimer only two out of four MD runs yielded the same result as before, namely that the carbon nanosheet is eventually inserted between the two monomers. In the two "successful" runs the insertion mechanism was a bit different, suggesting that one monomer could also be pulled above the carbon nanosheet, while the other one was kept at the nanosheet edge before being eventually adsorbed at the opposite side after a longer time related with the overall lengthy tilting of the monomer. Interestingly, when the insertion was eventually achieved the two barrel structures were again found to be parallel as found after adsorption on graphene, while the adsorption was again driven by the same hydrophobic residues responsible for the dimer interaction in the native state. An issue of great interest is that the interaction free energy showed a less favorable interaction on graphyne than on graphene for the same protein: this feature was attributed to the weaker dispersion (van der Waals) interactions on graphyne due to the smaller C atoms density of the latter material because of the acetylene linkers.

The problem of the possible effect of carbon nanomaterials on protein aggregation was also investigated by simulating the possible effect due to the use of CNT as drug delivery system on the cell biological functions related with filamentous actin (F-actin) affecting *inter alia* cell migration or proliferation and differentiation. In the cell, actin can be present as a free monomeric globular actin (G-actin), that can assemble into the microfilament structure. Since CNT were reported to affect the F-actin structure in a cell [47], the interaction of an actin trimer containing three G-actin monomers (an intermediate state in actin polymerization) with CNT was modeled by MD simulations [48]. The selected CNT was an armchair (5, 5) CNT with a dimeter 0.68 nm, while the tree G-actin monomers were in close contact, two being in the axial direction of the filament (the proximal monomers that could best interact with nanotube) and the third one (the distal monomer) farther from the nanotube. Three orientations of the CNT were therefore considered after preliminary docking trials. The first one, having the CNT aligned with the axis filament, yielded the most favorable interaction energy, whereas the other two, roughly orthogonal to the first one, showed weaker, but still favorable interactions, even though in one case full equilibration may not have been achieved. In the preferred geometry, 50% of the residues in proximity of the CNT were hydrophobic, unlike the majority of the surface residues of actin. In particular, van der Waals and π-π stacking led to strong interactions. As a result, the interaction between the two proximal actin monomers and that between one proximal and one distal monomer were enhanced compared to the control simulation with no CNT. Also the other interaction geometries affected to some extent the interaction strength among the monomers, and in one particular case the detachment of the distal monomer was observed due to a twist of CNT normal to its axis, thereby colliding with the trimer arrangement. Moreover, a significant motion of the CNT in contact with the actin trimer involving both translation along and rotation around the nanotube axis, related with the thermal fluctuations of the surface residues of actin. In conclusion, interaction with CNT did affect the intermonomer interaction within an actin filament by either increasing of decreasing its strength, henceforth also the actin-related cytoskeletal reorganization.

Concluding remarks and outlook to future simulations

The classical atomistic MD simulations are providing a large and continuously increasing amount of detailed information about the interaction of proteins on carbon nanomaterials, and in general of biological macromolecules and nanostructured materials. As previously noted when discussing some simulations, one important issue that should always be considered is the length of the simulation runs and the achievement of a true equilibrium state, rather than a metastable one. In fact in macromolecules such as the proteins, the overall relaxation of the long and structured backbone is quite lengthy and may proceed in a stepwise process related for instance to the local denaturation of the secondary structure. Moreover, the simulations in water do properly account for the hydration of the proteins and of the surface, but pose further problems, since the final adsorbed state requires a quite lengthy de-hydration process of the protein envelope and of the surface, even if the latter is highly hydrophobic, as first shown and discussed at length for lysozyme on crystalline polyethylene [49].

Another problem related with current force fields that may potentially affect the modeling of the protein-surface interaction in particular with carbon nanomaterials is the lack of explicitly accounting for the polarizability of delocalized π electrons. Such polarization is involved for instance in the π-π stacking interactions, but in this case an appropriate parametrization of the Lennard-Jones potential for sp^2 C atoms of the facing aromatic rings appears to produce good results in all force fields. On the other hand, there are the

interactions between electrically charged atoms or groups and the surface π electrons that may be more problematic to be properly parametrized, in particular using the usual Lorentz–Berthélot combination rules. In this case, the issue appears to be less problematic for the case of the charged Arg, Asp, Glu and to some extent Lys because of the charge delocalization, but it is potentially more worrying in the case of metal cations, if present, because the localized charge produces a quite strong electric field. The force fields appear in general to perform well with charged residues, in particular with Arg and Lys thanks also to the favorable contribution of the hydrophobic alkyl chains connecting the charged groups to the protein backbone, but this effect should be critically considered whenever metal ions are present.

Apart from these technical considerations, some general conclusions can already be drawn from the current MD simulations of protein adsorption on carbon nanomaterial surfaces. The nanomaterial surface curvature can be relevant whenever the radius of curvature is of the same order of magnitude as the protein size [7,15]. Thus, in general the 0-dimensional carbon fullerenes do not largely modify the overall protein structures, but they may occupy their active sites thus strongly affecting their biological functionality, as suggested in Refs. [8–14]. On the other hand, the surface concavity or convexity of typical 1-dimensional carbon nanotubes may differently affect protein adsorption. In particular, convex surfaces with increasingly larger radii of curvature lead to an increasingly stronger adsorption [15,18], so that it becomes largest on flat 2-dimensional graphene. Conversely, adsorption turns out to be stronger on the inner concave surface of carbon nanotubes with a decreasing, though still quite large, radius of curvature [15] because a smaller protein strain can be implicated. These features may also turn out to be also relevant in other nanomaterials when considering adsorption at nanoterraces or more generally near nanodefects leading for instance to a concave surface.

Another important issue emerging from the previously discussed papers is that charged basic residues, namely arginine and lysine, strongly enhance protein adsorption on graphene and in general on carbon nanomaterial surfaces [21]. This interaction is at least as strong as that shown by the aromatic residues (see also ref. [23]), and most likely even stronger in the case of arginine, a result that was already found, but not clearly stressed or even noticed previously (see Refs. [8,14,15]). The very favorable arginine adsorption was attributed in part to the dispersive interactions of the alkyl chain with the hydrophobic surface, but largely to the planarity of the guanidine moiety [21], where moreover the positive charge is delocalized on a few atoms: this planarity allows for a good interaction with the planar surface (or more generally with the planar aromatic rings of the surface), while still with only a minor decrease of the guanidine hydration. As a result, it turns out that the overall interaction strength is at least as large as that found for the π-π stacking interactions of the aromatic residues with the surface.

A further result that is beginning to emerge from the computer simulations of supramolecular protein complexes interacting with nanomaterials is that the latter ones may also affect the proteins' functionality by simply disrupting the aggregates, for instance by intercalation between dimeric proteins [45,46] within their hydrophobic interface. This is a further mechanism of interaction with proteins shown by carbon nanomaterials, in addition to the more familiar ones whereby they may occupy the protein active site or modify their secondary and tertiary structure. It should also be noted in this context that the effect of carbon nanomaterials inhibiting the aggregation of oligopeptides into amyloid fibrils with a β-sheet or β-barrel structure involved in the Alzheimer's disease [41–44] is clearly of great interest for its potential use, so that we may expect much further work in this area.

Let us conclude by saying that we expect an increasingly larger number of computer simulations, likely considering even larger systems or longer time spans modeling both functionalized systems increasingly closer to the experimental samples and additional proteins, but possibly tackling also more complicated systems with molecules of different nature. In this context, we limit ourselves to mention the case of different proteins that may adsorb on a given surface either sequentially [50], or competitively. In the latter case, one can hopefully model the faster diffusion of smaller proteins that may interact sooner with the surface and remain irreversibly adsorbed, or be replaced by larger ones if they have a larger affinity, thus modeling from first principles the Vroman effect [51].

Conflict of interest statement

Nothing declared.

References

Papers of particular interest, published within the period of review, have been highlighted as:

- • of special interest
- •• of outstanding interest

1. Lacerda L, Bianco A, Prato M, Kostarelos K: **Carbon nanotubes as nanomedicines: from toxicology to pharmacology**. *Adv Drug Deliv Rev* 2006, **58**:1460–1470.
2. Calvaresi M, Zerbetto F: **The devil and holy water: protein and carbon nanotube hybrids**. *Accounts Chem Res* 2013, **46**: 2454–2463.
3. Jimenez-Cruz CA, Kang Sg, Zhou R: **Large scale molecular simulations of nanotoxicity**. *WIREs Syst Biol Med* 2014, **6**: 329–343.
4. Yanamala N, Kagan VE, Shvedova AA: **Molecular modeling in structural nano-toxicology: interactions of nano-particles**

with nano-machinery of cells. *Adv Drug Deliv Rev* 2013, **65**: 2070–2077.

5. Zuo G, Kang Sg, Xiu P, Zhao Y, Zhou R: **Interactions between proteins and carbon-based nanoparticles: exploring the origin of nanotoxicity at the molecular level**. *Small* 2013, **9**: 1546–1556.

6. Antonucci A, Kupis-Rozmysłowicz J, Boghossian AA: **Noncovalent protein and peptide functionalization of single-walled carbon nanotubes for biodelivery and optical sensing applications**. *ACS Appl Mater Interfaces* 2017, **9**: 11321–11331.

7. De Leo F, Magistrato A, Bonifazi D: **Interfacing proteins with graphitic nanomaterials: from spontaneous attraction to tailored assemblies**. *Chem Soc Rev* 2015, **44**:6916–6953.

8. •• Calvaresi M, Zerbetto F: **Baiting proteins with C_{60}**. *ACS Nano* 2010, **4**:2283–2299.
An advanced docking procedure that allows for a fast screening of the interactions of a fullerene with an extensive protein data base and ranking the resulting complexes with good statistical results.

9. Calvaresi M, Zerbetto F: **Fullerene sorting proteins**. *Nanoscale* 2011, **3**:2873–2881.

10. Gao Z, Li H, Zhang H, Liu X, Kang L, Luo X, Zhu W, Chen K, Wang X, Jiang H: **PDTD: a web-accessible protein database for drug target identification**. *BMC Bioinf* 2008, **9**:104.

11. • Calvaresi M, Furini S, Domene C, Bottoni A, Zerbetto F: **Blocking the passage: C_{60} geometrically clogs K^+ channels**. *ACS Nano* 2015, **9**:4827–4834.
The thermodynamics of binding of fullerene inside the K+ channel allows to clearly describe the blocking mechanism both from the extra- and from the intra-cellular side.

12. Yang ST, Wang H, Guo L, Gao Y, Liu Y, Cao A: **Interaction of fullerenol with lysozyme investigated by experimental and computational approaches**. *Nanotechnology* 2018, **19**:395101.

13. Calvaresi M, Arnesano F, Bonacchi S, Bottoni A, Calò V, Conte S, Falini G, Fermani S, Losacco M, Montalti M, Natile G, Prodi L, Sparla F, Zerbetto F: **C_{60}@Lysozyme: direct observation by nuclear magnetic resonance of a 1:1 fullerene protein adduct**. *ACS Nano* 2014, **8**:1871–1877.

14. • Calvaresi M, Bottoni A, Zerbetto F: **Thermodynamics of binding between proteins and carbon nanoparticles: the case of C_{60}@Lysozyme**. *J Phys Chem C* 2015, **119**:28077–28082.
The thermodynamics of binding of fullerene with lysozyme showed the relevance of the van der Waals interactions together with the solvation and the entropy contributions, as well as the relevance of the aromatic and charged residues.

15. Raffaini G, Ganazzoli F: **Surface topography effects in protein adsorption on nanostructured carbon allotropes**. *Langmuir* 2013, **29**:4883–4893.

16. •• Saint-Cricq M, Carrete J, Gaboriaud C, Gravel E, Doris E, Thielens N, Mingo N, Ling WL: **Human immune protein C1q selectively disaggregates carbon nanotubes**. *Nano Lett* 2017, **17**:3409–3415.
A combination of computer simulations and analytical methods suggest that proteins may solubilize large nanotubes, whereas the small ones can be solubilzed only as whole bundles.

17. Israelachvili J: *Intermolecular and surface forces*. London: Academic Press; 1992. Chap. 11, par. 11.1.

18. Gu Z, Yang Z, Chong Y, Ge C, Weber JK, Bell DR, Zhou R: **Surface curvature relation to protein adsorption for carbon-based nanomaterials**. *Sci Rep* 2015, **5**:10886.

19. • Gao J, Wang L, Kang S, Zhao L, Ji M, Chen C, Zhao Y, Zhou R, Li J: **Size-dependent impact of CNTs on dynamic properties of calmodulin**. *Nanoscale* 2014, **6**:12828–12837.
This paper shows that carbon nanotubes may affect the physiological behavior of a protein also by affecting its intramolecular dynamic behavior.

20. Feng M, Bell DR, Luo J, Zhou R: **Impact of graphyne on structural and dynamical properties of calmodulin**. *Phys Chem Chem Phys* 2017, **19**:10187–10195.

21. •• Gu Z, Yang Z, Wang L, Zhou H, Jimenez-Cruz CA, Zhou R: **The role of basic residues in the adsorption of blood proteins onto the graphene surface**. *Sci Rep* 2015, **5**:10873.
Extensive molecular dynamics simulations show that charged basic aminoacids, namely Arg and Lys, are at least as important as aromatic ones in the protein interaction with hydrophobic carbon surfaces, while remaining also satisfactory hydrated.

22. Zhou R, Gao H: **Cytotoxicity of graphene: recent advances and future perspective**. *WIREs Nanomed Nanobiotechnol* 2014, **6**:452–474.

23. Camden AN, Barr SA, Berry RJ: **Simulations of peptide-graphene interactions in explicit water**. *J Phys Chem B* 2013, **117**:10691–10697.

24. Chong Y, Ge C, Yang Z, Garate JA, Gu Z, Weber JK, Liu J, Zhou R: **Reduced cytotoxicity of graphene nanosheets mediated by blood-protein coating**. *ACS Nano* 2015, **9**: 5713–5724.

25. • Zhao D, Li L, He D, Zhou J: **Molecular dynamics simulations of conformation changes of HIV-1 regulatory protein on graphene**. *Appl Surf Sci* 2016, **377**:324–334.
A paper showing that an α-helical oligopeptide can temporarily form a short antiparallel β-sheet, even though this structure was not stable for a long time and did not propagate.

26. Zhang M, Mao X, Wang C, Zeng W, Zhang C, Li Z, Fang Y, Yang Y, Liang W, Wang C: **The effect of graphene oxide on conformation change, aggregation and cytotoxicity of HIV-1 regulatory protein (Vpr)**. *Biomaterials* 2013, **34**:1383–1390.

27. Guo J, Yao X, Ning L, Wang Q, Liu H: **The adsorption mechanism and induced conformational changes of three typical proteins with different secondary structural features on graphene**. *RSC Adv* 2014, **4**:9953–9962.

28. • Raffaini G, Ganazzoli F: **Separation of chiral nanotubes with an opposite handedness by chiraloligopeptide adsorption: a molecular dynamics study**. *J Chromatogr A* 2015, **1425**: 221–230.
This paper indicates that chiral oligopeptide can discriminate between enantiomeric chiral nanotubes both on the outer and on the inner surface.

29. Roccatano D, Sarukhanyan E, Zangi R: **Adsorption mechanism of an antimicrobial peptide on carbonaceous surfaces: a molecular dynamics study**. *J Chem Phys* 2017, **146**, 074703.

30. Friedman SH, DeCamp DL, Sijbesma RP, Srdanov G, Wudl F, Kenyon GL: **Inhibition of the HIV-1 protease by fullerene derivatives: model building studies and experimental verification**. *J Am Chem Soc* 1993, **115**:6506–6509.

31. Ahmed L, Rasulev B, Turabekova M, Leszczynska D, Leszczynski J: **Receptor- and ligand-based study of fullerene analogues: comprehensive computational approach including quantum-chemical, QSAR and molecular docking simulations**. *Org Biomol Chem* 2013, **11**:5798–5808.

32. • Ahmed L, Rasulev B, Kar S, Krupa P, Mozolewska MA, Leszczynski J: **Inhibitors or toxins? Large library target-specific screening of fullerene-based nanoparticles for drug design purpose**. *Nanoscale* 2017, **9**:10263–10276.
The screening procedure proposed in ref. 8 was extended to functionalized fullerenes and to pristine fullerenes of different sizes.

33. Radic S, Nedumpully-Govindan P, Chen R, Salonen E, Brown JM, Ke PC, Ding F: **Effect of fullerenol surface chemistry on nanoparticle binding-induced protein misfolding**. *Nanoscale* 2014, **6**:8340–8349.

34. Yu Y, Sun H, Hou T, Wang S, Li Y: **Fullerene derivatives act as inhibitors of leukocyte common antigen based on molecular dynamics simulations**. *RSC Adv* 2018, **8**:13997–14008.

35. Zhang Y, Jimenez-Cruz CA, Wang J, Zhou B, Yang Z, Zhou R: **Bio-mimicking of proline-rich motif applied to carbon nanotube reveals unexpected subtleties underlying nanoparticle functionalization**. *Sci Rep* 2014, **4**:7229.

36. Zuo G, Gu W, Fang H, Zhou R: **Carbon nanotube wins the competitive binding over proline-rich motif ligand on SH3 domain**. *J Phys Chem C* 2011, **115**:12322–12328.

37. • Sun J, Du K, Fu L, Gao J, Zhang H, Feng W, Ji P: **Sodium hexadecyl sulfate as an interfacial substance adjusting the adsorption of a protein on carbon nanotubes**. *ACS Appl Mater Interfaces* 2014, **6**:15132–15139.
Carbon nanotubes can be solubilized in water when non-covalently coated with surfactants, and this paper investigates lysozyme adsorption on this nanotube-surfactant system.

38. Baweja L, Balamurugan K, Subramanian V, Dhawan A: **Hydration patterns of graphene-based nanomaterials (GBNMs) play a major role in the stability of a helical protein: a molecular dynamics simulation study**. *Langmuir* 2013, **29**: 14230–14238.

39. • Sun X, Feng Z, Hou T, Li Y: **Mechanism of graphene oxide as an enzyme inhibitor from molecular dynamics simulations**. *ACS Appl Mater Interfaces* 2014, **6**:7153–7163.
Graphene oxide has a strong inhibitory effect on α-chymotrypsin, and this paper investigates the reasons of this behavior, suggesting also that pristine graphene should not affect the enzyme behavior, unlike its oxidized form.

40. Zhao D, Li L, Zhou J: **Simulation insight into the cytochrome c adsorption on graphene and graphene oxide surfaces**. *Appl Surf Sci* 2018, **428**:825–834.

41. Fu Z, Luo Y, Derreumaux P, Wei G: **Induced β-barrel formation of the Alzheimer's aβ25–35 oligomers on carbon nanotube surfaces: implication for amyloid fibril inhibition**. *Biophys J* 2009, **97**:1795–1803.

42. Li H, Luo Y, Derreumaux P, Wei G: **Carbon nanotube inhibits the formation of β-sheet-rich oligomers of the Alzheimer's amyloid-β(16-22**. *Pept Biophys J* 2011, **101**:2267–2276.

43. Xie L, Luo Y, Lin D, Xi W, Yang X, Wei G: **The molecular mechanism of fullerene-inhibited aggregation of Alzheimer's β-amyloid peptide fragment**. *Nanoscale* 2014, **6**: 9752–9762.

44. Xie L, Lin D, Luo Y, Li H, Yang X, Wei G: **Effects of hydroxylated carbon nanotubes on the aggregation of aβ16–22 peptides: a combined simulation and experimental study**. *Biophys J* 2014, **107**:1930–1938.

45. • Luan B, Huynh T, Zhao L, Zhou R: **Potential toxicity of graphene to cell functions *via* disrupting protein-protein interactions**. *ACS Nano* 2015, **9**:663–669.
Dimeric proteins interacting through a hydrophobic interface could be sparated by graphene intercalation, as suggested by these molecular dynamic simulations.

46. Luan B, Huynh T, Zhou R: **Potential interference of Protein–Protein interactions by graphyne**. *J Phys Chem B* 2016, **120**:2124–2131.

47. Holt BD, Shams H, Horst TA, Basu S, Rape AD, Wang Y-L, Rohde GK, Mofrad MRK, Islam MF, Dahl KN: **Altered cell mechanics from the inside: dispersed single wall carbon nanotubes integrate with and restructure actin**. *J Funct Biomater* 2012, **3**:398–417.

48. Shams H, Holt BD, Mahboobi SH, Jahed Z, Islam MF, Dahl KN, Mofrad MRK: **Actin reorganization through dynamic interactions with single-wall carbon nanotubes**. *ACS Nano* 2014, **8**:188–197.

49. Wei T, Carignano MA, Szleifer I: **Lysozyme adsorption on polyethylene surfaces: why are long simulations needed?** *Langmuir* 2011, **27**:12074–12081.

50. Raffaini G, Ganazzoli F: **Sequential adsorption of proteins and the surface modification of biomaterials: a molecular dynamics study**. *J Mater Sci Mater Med* 2007, **18**:309–316.

51. Vroman L, Adams AL, Fischer GC, Munoz PC: **Interaction of high molecular weight kininogen, factor XII, and fibrinogen in plasma at interfaces**. *Blood* 1980, **55**:156–159.